Published in final edited form as:
J Immunol. 2012 October 1; 189(7): 3767–3776. doi:10.4049/jimmunol.1201216.

Inducible tertiary lymphoid structures, autoimmunity and exocrine dysfunction in a novel model of salivary gland inflammation in C57BL/6 mice§

Michele Bombardieri[*,1], **Francesca Barone**[*,2], **Davide Lucchesi**[1], **Saba Nayar**[2], **Wim B van den Berg**[3], **Gordon Proctor**[4], **Christopher D Buckley**[2], and **Costantino Pitzalis**[1]

[1]Centre for Experimental Medicine and Rheumatology, William Harvey Research Institute, Queen Mary University of London, London, United Kingdom [2]Rheumatology Research Group, University of Birmingham, Birmingham, United Kingdom [3]Department of Rheumatology, Radboud University Medical Centre, Nijmegen, The Netherlands [4]Oral Medicine and Pathology, King's College, London, United Kingdom

Abstract

Salivary glands in patients with Sjögren's syndrome (SS) develop ectopic lymphoid structures (ELS) characterized by B/T cell compartmentalization, the formation of high endothelial venules (HEV), follicular dendritic cell networks (FDCs), functional B cell activation with expression of activation-induced cytidine deaminase (AID) as well as local differentiation of autoreactive plasma cells. The mechanisms triggering ELS formation, autoimmunity and exocrine dysfunction in SS are largely unknown. Here we present a novel model of inducible ectopic lymphoid tissue formation, breach of humoral self-tolerance and salivary hypofunction following delivery of a replication-deficient adenovirus-5 (AdV5) in submandibular glands of C57BL/6 mice through retrograde excretory duct cannulation. In this model, inflammation rapidly and consistently evolves from diffuse infiltration towards the development of SS-like periductal lymphoid aggregates within 2 weeks from AdV delivery. These infiltrates progressively acquire ELS features and support functional GL7+/AID+ germinal centers. Formation of ELS is preceded by ectopic expression of lymphoid chemokines CXCL13, CCL19 and lymphotoxin-β and is associated with development of anti-nuclear antibodies in up to 75% of mice. Finally, reduction in salivary flow was observed over 3 weeks post AdV infection consistent with exocrine gland dysfunction as a consequence of the inflammatory response. This novel model has the potential to unravel the cellular and molecular mechanisms regulating ELS formation and their role in exocrine dysfunction and autoimmunity in SS.

INTRODUCTION

The formation of ectopic lymphoid structures (ELS), defined as aggregates of lymphoid cells forming ectopically in non-lymphoid locations and characterized by B/T cell

§MB is recipient of a Clinician Scientist Fellowship from the Arthritis Research UK (grant 18237). FB is recipient of a Clinician Scientist Fellowship from the Wellcome Trust.

Corresponding Authors: Dr Michele Bombardieri Centre for Experimental Medicine & Rheumatology, William Harvey Research Institute, Queen Mary University of London, Charterhouse Square, London EC1M 6BQ, UK Tel: +44 (0)2078828193 Fax:+44 (0)2078828250 m.bombardieri@qmul.ac.uk; Dr. Francesca Barone School of Immunity and Infection, MRC Centre for Immune Regulation College of Medical and Dental Sciences, University of Birmingham Edgbaston, BirminghamB15 2TT, UK Tel +44 (0)1214146780 Fax +44 (0)1214145475 f.barone@bham.ac.uk.
*The first two Authors contributed equally

Europe PMC Funders Author Manuscripts

segregation, differentiation of high endothelial venules (HEV) and development of follicular dendritic cells (FDC) networks supporting a germinal center response has been observed in chronic inflammatory conditions of both autoimmune and microbial origin (1-3). In Sjögren's syndrome (SS), a chronic autoimmune disease characterised by circulating high affinity, class switched autoantibodies against nuclear antigens and ribonucleoproteins such as Ro/SSA and La/SSB (4) and development of oral and ocular dryness (sicca syndrome) resulting from immune cell infiltration in the exocrine glands (5), salivary ELS develop in 30-40% of patients (6, 7). The development of ELS in SS is thought to be regulated by the ectopic production of lymphoid chemokines CXCL13 and CCL21 (7-9) which physiologically regulate the recirculation and positioning of CXCR5+ and CCR7+ immune cells within secondary lymphoid organs (SLO). Recently, we and others have shown that ELS in SS salivary glands acquire structures typical of germinal centers in SLOs and are capable of supporting the selection and expansion of autoreactive B cell clones as demonstrated by local expression of AID and differentiation of autoreactive plasma cells (10-12). Moreover, prospective data in a large cohort of SS patients provided evidence that the presence of ELS in the salivary glands is an independent predictor of a more aggressive disease phenotype and development of salivary B cell lymphomas (13), suggesting that ELS exert a central pathogenic role in SS and might represent a potential therapeutic target. However, our current understanding of the key cellular and molecular events triggering and regulating the formation of ELS in the salivary glands is inadequate and limited to cross-sectional analysis in SS patients and spontaneous murine models of SS such as NOD mice (14). In addition, it is also unclear why ELS form in some patients but not others and whether these represent discrete disease subsets driven by different triggering agents or different evolutionary stages (15). Here we present a new inducible model of sialoadenitis developing in the salivary glands of wild-type C57BL/6 animals in response to selective submandibular gland administration of a replication-defective adenovirus 5 (AdV5) which recapitulates several features of SS, such as formation of ELS, ectopic expression of lymphoid chemokines and functional B cell activation. Importantly, not only AdV5 infection reproduces the phenotypic features of SS, but also functionally leads to the development of humoral autoimmunity to nuclear antigens and decrease in salivary flow. Thus, this novel model offers the unique possibility to dissect the cellular and molecular mechanisms regulating breach of tolerance, autoimmunity and ELS formation in the salivary glands.

MATERIALS AND METHODS

Animal collection

All procedures were performed with approval from the local Animal Ethics and Welfare Committee and under a Home Office project license according to Home Office regulations (LREC). Young adult female C57BL/ 6 (Harlan Labs Ltd., Loughborough, UK), aged between 10-13 weeks at the start of the experiments, were housed under standard conditions.

Adenovirus preparation and intra-salivary gland delivery

Concentrated stocks of E1-E3 replication-deficient human AdV5 encoding for firefly luciferase (LucAdV), generated and characterized as previously described (16) or for bacterial beta-galactosidase (LacZAdV, a kind gift of Dr Gnudi, KCL, UK) were used to produce bulk amount of viral particles via Hek293 cells infection followed by purification using a discontinuous CsCl gradient. AdV were then dialyzed against a solution containing 1 mM MgCl2, 10 mM Tris (pH 7.4), and 150 mM NaCl with 10% glycerol (vol/vol) overnight on a Side-a-lyzer dialysis cassette (Slide-A-Lyzer 3.5K MWCO, Thermo Scientific). AdV particles collected from dialysis cassette were titrated using plaque forming assay method and 50% Tissue Culture Infective Dose (TCID50) according to the statistical method devised by Reed and Muench (17). Retrograde mouse submandibular excretory duct

cannulation was performed as described previously in rats, with minor modifications (18). Briefly, mice were anaesthetized with ketamine (60 mg/kg) and xylazine (12 mg/kg) i.p. and then the submandibular gland was cannulated through the excretory duct using heat-drawn glass gas chromatography tubing (0.1 mm i.d.; Sigma Ltd). Approximately 20 μl of adenovirus solution (see below), equivalent to 1×10^8 pfu of reporter-encoding AdV or buffer vehicle were injected into the submandibular gland using an attached Hamilton syringe (Sigma Ltd). The same volume of the vehicle buffer was delivered as negative control.

Mice were culled under terminal anesthesia at days 4, 7 (grouped as week 1), 11, 14 (week 2), and 18, 21 (week 3) post-cannulation (pc). A minimum of 5 mice per time point was used. Submandibular gland and draining lymph nodes were removed and partly snap-frozen in OCT (Sakura Finetek, Thatcham, UK) for cryosectioning and partly stored in RNA Later (Ambion, UK) for gene expression profiling.

Detection of luciferase and beta-galactosidase activity in the salivary glands

For Luciferase assay, LucAdV cannulated glands were lysed in GloLysis buffer (Promega) using a micro-beads homogeniser (Precellys System, Bertin Technologies). Lysates were then assayed with BrightGlo substrate (Promega) according to manufacturer's instructions. Luciferase activity over 10 seconds was measured in a microplate luminometer (Microlumat Plus, EG&G Berthold). Luciferase activity values were normalised against the protein concentration of the lysate measured with a BCA protein assay kit (Pierce).

For beta-galactosidase detection, LacZAdV-injected glands were snap-frozen in OCT for cryosectioning. Six-μm thick sections were cut on microscope slides and fixed in 2% PFA. Sections were then incubated with complete X-gal substrate (Sigma) at 37°C overnight, washed twice in PBS and counter-stained in haematoxylin. Slides were then mounted and observed under light microscope.

Submandibular gland histomorphology

Immune cell infiltrate organization and ELS formation in the submandibular glands were characterized by routine staining with H&E to define the presence and prevalence of inflammatory infiltrates. Periductal foci defined as the presence of more than 50 periductal infiltrating leukocytes were analysed at 3 different cutting levels at 50 μm intervals.

Characterization of ELS in cannulated salivary glands

The presence of ELS was characterised by immunofluorescence for the presence of T/B cell segregation, PNAd+ HEV, development of FDC networks and differentiation of germinal-center B cells, as previously described (19). For T/B cell segregation, first, sections were double stained for CD3/B220 at 3 cutting levels 100μm apart in order to have a representative coverage of each aggregate; second, stained slides were assessed blindly by two independent observers. T/B cell segregation was defined when both observers agreed on the presence of full and/or partial aggregation of T and B cells in diverse areas in at least 2 of the 3 cutting levels. Aggregates which did not fulfil this definition were considered as non-segregated. Double staining for B220/GL7 was performed to identify germinal center B cells while FDC-M1 was used on sequential sections to evaluate the presence of FDC networks. Finally, for HEV identification and lymphangiogenesis, salivary glands were double-stained for peripheral node addressin (Meca-79) (see also Supplementary Table I and Figure 3 for HEV colocalization within the T cell area) and lymphatics (LYVE-1). For the lymphoid chemokine (CXCL13 and CCL21) staining, first endogenous biotin was blocked with preincubation with avidin and biotin, samples were then blocked with 10% horse serum in PBS and incubated with CXCL13 or CCL21, CD3 and CD19 for one hour. After

washing, slides were incubated with appropriate secondary and tertiary antibodies or streptavidin for 30 mins, washed and mounted with Prolog Gold (−). All secondary antibodies were pre-adsorbed in 10% mouse serum for 30 min prior to incubation. Staining was carried out in moist chambers at room temperature. Images were acquired on a Zeiss Confocal Microscope and LSM510 Image Examiner Software was used to process the pictures obtained. A list of the antibodies used for immunofluorescence is presented in Table I and Supplementary Table I.

Gene expression profiling of ELS-related genes in the salivary glands

Total RNA was extracted from submandibular glands using the RNeasy Mini kit (Qiagen), with on column DNase I digestion to avoid genomic DNA contamination. RT-PCR ThermoScript System for first-strand cDNA synthesis (Invitrogen Life Technologies) was used to produce cDNA from 1 mg of total RNA. Primers and probes for quantitative Taqman real-time evaluation of CXCL13, CCL19, CXCR5, CCR7, Ltβ, LtβR, AID, BAFF, IL-4 and IL-21 were obtained from Applied Biosystems (Table II). Samples were run in triplicate at 10 ng of cDNA/well, detected using the ABI PRISM 7900HT instrument and results analyzed using the ABI PRISM 7900HT sequence detection system version 2.1. Relative quantification was assessed using the comparative CT (threshold cycle) method with cDNA from vehicle-cannulated glands used as calibrator.

Assessment of Salivary Exocrine Function

Secretory function was assessed in AdV-treated and contralateral submandibular gland under terminal anesthesia (pentobarbitone 75 mg/kg i.p.). Each submandibular duct was exposed by dissection from the ventral surface through the mylohyoid muscle. Individual submandibular ducts were cut, cannulated and saliva collected for 10 min following onset of secretion after stimulation with pilocarpine (0.5mg/kg i.p.). Following collection into weighed Eppendorf tubes the tubes were re-weighed and the volume of saliva calculated (1mg = 1μl saliva). Results were expressed as mg saliva/10 min/g body weight.

Anti-Nuclear Antibodies (ANA) detection

Twelve-spot microscope slides (CA Hendley, Essex, UK) were seeded with Hep-2 cells at 5×10^4 cells/well and left in culture overnight. When ready, slides were washed in PBS and fixed in acetone. Animal sera were serially diluted in PBS (1:80, 1:160, 1:320) and 15ml of diluted serum were deposited on each well. Serial dilutions of pooled sera from anti-nuclear antibodies positive animals (MRL/lpr mice) were used as positive controls. Sample and control sera were incubated for 1 hour at room temperature, washed twice in PBS and incubated with FITC anti-mouse IgG (Sigma, Poole, UK) for 30 minutes in the dark. Slides were washed twice in PBS, mounted and observed at fluorescence microscope for anti-nuclear antibodies staining.

Detection of anti-AdV antibodies by Western Blot

To assess the production of anti-viral antibodies in sera of AdV-cannulated mice at different time points, LucAdV or LacZAdV-infected (or untreated) HEK293 cells were lysed in RIPA buffer and the protein concentration was determined by BCA assay (Pierce, UK). A total of 25μg/lane of the different lysates were separated by SDS-PAGE on a 4-12% Novex polyacrylamide gel (Invitrogen, UK) and transferred on nitrocellulose membrane using an iBlot device (Invitrogen, UK) following manufacturer's instructions. Membrane strips were blocked with 5% milk in TBST for 4h at RT and then incubated with individual serum from AdV- or vehicle-treated mice(at 5, 9, 12, 15, 20, 23 days) diluted 1:100 in block buffer over-night at 4°C. A rabbit anti-AdV antiserum (Abcam, UK) was used as positive control. Membrane strips were then incubated with HRP-conjugated anti-mouse (Sigma, Poole, UK)

or anti-rabbit (DAKO, UK) IgG antibody and peroxidase activity was visualized using ECL reagents (Amersham, UK) following manufacturer's instructions.

Statistical Analysis

Differences in quantitative variables were analyzed by the Mann-Whitney U test when comparing two groups and by the Kruskal-Wallis with Dunn's post-test when comparing multiple groups. $\chi 2$ test with Yates' correction when required or Fisher's exact test when appropriate were used to evaluate associations of qualitative variables in the different groups. All the statistical analyses were performed using GraphPad Prism version 5.01 for Windows (GraphPad, San Diego, CA). A p value <0.05 was considered statistically significant.

RESULTS

Dose-response time course analysis of AdV gene transfer

Delivery of replication deficient AdV5 in murine submandibular salivary glands via retro-cannulation of the excretory duct has previously been described as a suitable and efficient tool for transient local gene transfer (20). We adapted a retrograde cannulation technique which we previously developed in rats (18) using customised glass cannulae and proved to be a reliable method for specific delivery of small volumes (up to 50μl) in the submandibular glands (Figure 1A,B). As shown in Figure 1C, this technique allows precise delivery and full permeation of the cannulated submandibular gland of C57B/6 mice but not the adjacent sublingual gland or the contralateral gland. Using this approach we next performed a time-course and dose-response analysis of gene transfer using a replication defective human adenovirus 5 (AdV), encoding for the firefly luciferase gene (LucAdV). As shown in Figure 1D, increasing luciferase activity was observed using increasing doses of LucAdV within the first week post-cannulation (pc), which then decreased over the next two weeks

Formation of SS-like aggregates in submandibular glands is dependent on AdV dose and lack of viral clearance in ductal epithelial cells

Histological analysis of the cannulated glands demonstrated that AdV doses of 10^8 pfu per gland, but not vehicle control (or doses <10^7 pfu, data not shown), induced from week 2 pc the formation of lymphomonocytic infiltrates organized as periductal aggregates which by week 3 pc strongly resembled lymphocytic foci found in SS patients (Figure 2 A-F).

The formation of lymphoid aggregates was invariably preceded by a rapidly induced diffuse inflammatory infiltrate, which resolved within the first week pc (Figure 2D and 2G) to be replaced by typical periductal focal infiltration by week 2 pc. Importantly, this phenomenon was independent from the reporter gene used, as it was also triggered by same amounts of LacZAdV (Figure 2 G-I) with no significant difference in terms of prevalence and size of the periductal foci comparing the two viruses. The mean ± SEM of the number of periductal foci developing in the salivary glands after delivery of either LucAdV or LacZAdV at the different time points is reported in Figure 2J.

The use of the LacZAdV, allowed us to investigate the relationship between viral localization and immune cell infiltration at the different time-points analysed. As shown in Figure 2 (G-I), staining for bacterial β-galactosidase demonstrated early widespread distribution of the virus within the gland (Figure 2G). By week 2 pc the LacZAdV was almost exclusively localized within ductal epithelial cells surrounded by initial inflammatory aggregates (Figure 2H). Confirmation of selective colocalization of AdV particles within ductal epithelial cells was demonstrated by double immunostaining with an anti-cytokeratin

antibody (Supplementary Figure 1). Although we could not detect residual β-galactosidase staining in ducts surrounded by large aggregates at week 3 pc (Figure 2I), luciferase activity was still detectable in all infiltrated glands at this time point (Figure 2K). Overall, in the presence of residual luciferase activity, from week 2 pc onwards, 100% of cannulated glands displayed focal periductal aggregates, demonstrating high reproducibility and disease penetrance of our model.

Focal lymphocytic infiltration following AdV delivery display progressive features of ELS: B/T cell segregation and development of FDC networks

We next evaluated the progressive acquisition of SLO features by the inflammatory foci, such as T/B cell segregation and differentiation of FDC networks. Double immunofluorescence sequential section analysis of submandibular gland infiltrates was performed using CD3/B220 and B220/FDC-M1 in order to assess the presence of T/B cell compartmentalization and FDC network formation (19). Initial infiltrates (week 1) were mostly diffuse and characterized by a predominance of T cell infiltration followed by a progressive influx of B cells and the development of highly organized lymphoid structures with T and B lymphocytes localizing in discrete areas (week 2-3)(Fig 3 A-C). Thus, upon AdV delivery T and B cells serially enter the glands first with a non-segregated pattern and then gradually develop an organized segregated disposition in up to 70% of the aggregates (Fig 3 G). Furthermore, we observed differentiation of FDC networks within the B cell rich areas in the context of segregated infiltrates in over60% of the mice at week 3 pc (Fig 3 D-F and H).

Ectopic expression of lymphoid chemokines

Production of lymphoid chemokines CXCL13, CCL21 and CCL19 is of pivotal importance in the development of ELS in chronic autoimmune diseases, including SS (2, 15). Induction and secretion of lymphoid chemokines has been shown to rely on the expression of the heterotrimeric lymphotoxin α1β2 (Ltβ) (21-23). To verify the involvement of these regulators of ELS in our model we assessed the ectopic expression of CXCL13 and CCL19 and their cognate receptors CXCR5 and CCR7 as well as the Ltβ/LtβR axis in the cannulated salivary glands.

A shown in Fig 4 (A-F), CXCL13/CXCR5 and CCL19/CCR7 mRNA transcripts were abundantly upregulated in AdV-treated mice, as compared to vehicle-treated mice, and their ectopic expression was consistent with the progressive detection of ELS in the salivary glands, reaching their peak of expression between week 2 and 3 pc. Of relevance, Ltβ, CXCL13/CXCR5 and CCL19/CCR7 mRNA displayed significant upregulation within the first week pc suggesting very early involvement of these factors in the formation of ELS in this inducible model of lymphoid neogenesis.

To confirm the presence and expression pattern of lymphoid chemokines at a protein level, we used multicolor confocal microscopy to detect CXCL13 or CCL21 together with B220/CD3. As shown in Figure 4 (G-N), in the context of segregated aggregates, CXCL13 and CCL21 retained their expression pattern within the B and T cell-rich areas respectively, suggesting a prominent role in directing T/B cell segregation.

Inducible ectopic lymphoid aggregates progressively acquire characteristic of functional germinal centers

We next assessed the presence of features typically associated with germinal center function such as differentiation of germinal center B cells and expression of AID. As shown in Figure 5, sequential section analysis (Figure 5 A-D) demonstrated that T/B segregated aggregates characterized by the differentiation of high-endothelial venules (HEV) in the T cell-rich area

(see also Supplementary Figure 3 for direct colocalization of HEV and T cells) and FDCs within the B cell follicle support the activation of numerous GL7+ germinal center B cells. The appearance of GL7+ germinal centers was strongly associated with functional B cell activation as demonstrated by the detection of high levels of mRNA transcripts for AID (Figure 5E), the enzyme required for Ig somatic hypermutation (SHM) and class-switch recombination (CSR). Of relevance, ectopic induction of AID was also associated with the expression of several cytokines which are known to co-operate in directly promoting AID expression in B cells, such as IL-4, BAFF and IL-21 (Figure 5 F-H). Overall, these data demonstrate that following AdV infection, ELS support the development of functional niches of B cells which acquire the machinery to undergo SHM and CSR at these ectopic sites.

Humoral immune response against AdV infection favors breach of tolerance against nuclear self-antigens

In patients with SS the formation of immune cells infiltrates in the salivary glands is associated with the presence of circulating autoantibodies against nuclear antigens and ribonucleoproteins (4, 24, 25). Thus, we next investigated whether this model of AdV-induced sialoadenitis was associated not only with the formation of anti-AdV antibodies but also with breach of self-immunological tolerance and development of antinuclear antibodies. As expected sera from AdV-cannulated mice but not control C57Bl/6 progressively displayed a strongly anti-viral activity appearing as early as day 5, with humoral responses prevalently directed against proteins of the viral core and the viral capside (Figure 6 A). The presence and titer of antinuclear antibodies was determined using Hep2 cells as substrate. We chose an initial serum dilution of 1:80 as this is considered significant in clinical tests for autoimmunity in patients. As shown in Figure 6 B-E, no sera from AdV-cannulated mice within week 1 pc displayed ANA positivity. Conversely, ANA reactivity was detected in 30.7% of mice by week 2 pc and this percentage increased to 75% in animals culled at week 3 pc. Interestingly, at week 3 pc the prevalence of ANA was higher in FDC+ vs FDC- mice (87.5% vs 25% respectively). Finally, age/sex-matched vehicle control C57Bl/6 mice did not show any reactivity.

Taken together these observations demonstrate that AdV-induced sialoadenitis in non-autoimmune prone mice is associated with the induction of humoral autoimmunity towards nuclear antigens.

AdV infection induces sustained reduction in salivary flow in the affected but not contralateral gland

SS patients are characterized by an excretory dysfunction of the salivary (and lacrimal) glands that leads to mouth (and eye) dryness, also denoted as *sicca* syndrome. In order to assess whether AdV-delivery induced exocrine dysfunction in the affected gland, each mouse were cannulated with 10^8pfu of AdV in one the submandibular glands and with vehicle control in the contralateral gland. At appropriate time-points post cannulation, pilocarpine-stimulated salivary flow was measured from each individual gland separately as described in the methods.

A significant and acute reduction in salivary flow (Figure 7) was observed within week 1 pc, in line with the histological evidence of diffuse epithelial cell apoptosis up to day 3 pc (Supplementary Figure 2). Surprisingly, albeit less drastic, at week 2 and week 3 pc a significant reduction in saliva production was still evident in AdV-treated mice characterized by the presence of lymphocytic aggregates in salivary glands with an otherwise reconstituted acinar and ductal architecture. This suggests that within the observed

period immune cell infiltration induces a functional impairment which does not allow the full recovery of the excretory function of the glands.

DISCUSSION

The formation of ELS in the target organ of several chronic inflammatory conditions, including SS, has long been recognized (1-3, 7, 26-28). ELS formation is highly relevant to SS as germinal center-like structures in the labial salivary glands are independent predictors of increased disease severity and evolution towards B cell lymphomas (6, 13).

The lack of reliable inducible animal models of ectopic lymphoid neogenesis has limited our understanding of the mechanisms leading to the formation of ELS in the salivary glands. Murine models of inducible sialoadenitis with some features of SS in response to systemic or local viral infection have been reported. However, in order to induce sialoadenitis previous work relied either on the use of fully infectious and replicating sialotropic viruses in autoimmune prone mice such as lpr/lpr mice (29, 30), or replication-deficient AdV vectors harboring genes encoding for pro-inflammatory mediators such as IL-17 (31). In addition, no comprehensive demonstration that viral-induced sialoadenitis can progress towards the formation of functional ELS and resemble the main physiopathological characteristic of SS (ie the formation of autoantibodies) has, to our knowledge, been as yet provided.

Here we present a novel model of inducible lymphoid neogenesis which rapidly develops in the submandibular glands of wild-type C57Bl/6 mice in response to local delivery of replication-deficient adenoviral vectors. In this model of sialoadenitis, immune cell infiltration rapidly progresses from a diffuse inflammatory process towards the formation of periductal lymphocytic aggregates which further evolve into highly organised ELS within 3 weeks from viral infection. This process is reproducible and synchronous with lymphocytic foci developing in 100% of the mice by week 2 pc and evolving by week 3 pc into fully formed ELS characterised in approximately 70% of the mice by T/B cell segregation and formation of FDC networks with germinal center-like structures with high similarity to the human counterpart (7).

The formation of ELS has been suggested to be the result of a tightly regulated series of immunological and molecular processes with recapitulation of the main pathways involved in lymphoid organogenesis in prenatal life (32). Embryonic lymphoid organ development is critically dependent on lymphoid chemokines CXCL13, CCL19 and CCL21 which are produced by VCAM-1+ICAM-1+LTβR+ mesenchymal “organizer” cells in response to close interaction with CD3-CD4+CD45+IL-7Ra+RANK+ lymphoid “inducer” cells (Lti) expressing the membrane-bound heterotrimeric (α1β2) member of TNF family lymphotoxin (LT) LTβ(32). The establishment of a positive feedback loop between lymphoid chemokines and LTβ is critical in promoting the development of the stromal and vascular architecture of SLOs, including the differentiation of HEVs (21).

However, evidence from transgenic models of ELS has questioned the relevance of Lti in ectopic lymphoid neogenesis in adult life (33). Similarly, lymphoid chemokine expression in patients with ELS developing during chronic inflammatory diseases, including SS (7-9, 11, 34), suggests that the lymphoid chemokines/LTβ pathway in inducible ELS formation is regulated by cellular and molecular mechanisms which are different from the conventional interactions observed during embryonic development.

Here we showed that following AdV delivery early up-regulation of lymphoid chemokines CXCL13, CCL19 and CCL21 mRNA precedes the development of ELS and peaks in concomitance with fully functional ELS. Of interests, lymphoid chemokines retained their

discrete expression pattern observed in SLOs, with CXCL13 confined to the B cell-rich areas of the periductal aggregates and CCL21 in the surrounding T cell area. This suggests that the progressive recruitment and positioning of T and B cells subsets following AdV infection in the salivary glands are not random events but follow tightly regulated chemoattractive gradients and establish this inducible model of ELS as a suitable platform to dissect the dynamic expression, source of production and hierarchical importance of the critical factors regulating ectopic lymphoid neogenesis.

Interestingly, we also found that in this model formation of ELS was invariably associated with the persistence of the transgene product within the salivary glands 3 weeks after AdV delivery, despite viral inability to replicate. Strikingly, prolonged viral and transgene protein expression was selectively observed within ductal epithelial cells, an observation in keeping with the inability of this cell type to clear viral pathogens as described both in rodent and human salivary glands (35, 36). This is relevant for SS since several viruses have been implicated in SS pathogenesis and a type-I interferon signature is typical of the disease (37, 38). Thus, in this model induction of ELS likely derives from lack of viral clearance resulting in prolonged antigenic exposure which is a potent trigger for ELS formation, as previously suggested in other models of ectopic lymphoid neogenesis such as chronic graft rejection (39) and autoimmune insulitis in NOD mice (19). Thus, we believe that this model has the potential to unravel the intimate physiopathological viral-host interactions leading to the formation of ELS in SS.

Importantly, in this work we have also demonstrated that AdV-induced ELS not only recapitulate the cellular and molecular organization of SLOs but also support functional B cell activation with expression of AID, the enzyme which initiates somatic hypermutation (SHM) and class switch recombination (CSR) of the Ig genes (40), leading to affinity maturation and differentiation of memory B and plasma cells (41, 42). Expression of AID in the salivary glands required the formation of ELS acquiring markers of germinal centers such as FDC networks and GL7, similarly to SS patients (10). AID expression and subsequent CSR in naïve B cells can be directly induced by a milieu of cytokines among which BAFF, IL-4, IL-10 and IL-21, even in the absence of B-cell receptor cross-linking (43-47). Accordingly, in this model AID transcript levels were strictly associated with the expression of BAFF, IL-4 and IL-21 mRNA suggesting a functional role for these factors in downstream B cell activation.

Because the architectural, cellular and molecular features of ELS in this model were highly reminiscent of those observed in SS, we next investigated whether typical features of the human disease were also present in this model. Two hallmarks of SS are the breach of self-immunological tolerance towards nuclear antigens with circulating autoantibodies and a progressive exocrine dysfunction which results in the classical signs and symptoms of mouth/eye dryness (sicca syndrome). At week 3 pc 75% of the AdV-cannulated mice developed positivity for IgG ANA, in comparison none of the vehicle controls displayed evidence of autoimmunity. Interestingly, onset of ANA was preceded by the rapid and abundant induction of epithelial cells apoptosis following AdV infection, as demonstrated by the presence of pyknotic nuclei and positive TUNEL staining (Supplementary Figure 2). It is likely that exposure of nuclear material in the context of the ectopic formation of B cell follicles in the salivary glands would be sufficient to trigger autoimmunity. In this regard, it will be interesting to dissect whether ELS are directly involved in the generation of autoantibodies over and above draining lymph nodes, as previously demonstrated for ELS in patients with SS (11, 12).

Finally, we showed that the development of sialoadenitis and ELS is also accompanied by exocrine dysfunction. Although we did not elucidate the pathophysiology of hypo-secretion

Europe PMC Funders Author Manuscripts

in this model, which might be due to viral and/or immune mediated mechanisms, our observations would be in keeping with indications in patients with SS that exocrinopathy in the context of focal sialoadenitis is primarily due to a functional rather than anatomical impairment (48).

In conclusion, we present a novel model of AdV-induced lymphoid neogenesis which has the potential to unravel the critical interactions between viral infection, formation of ELS, breach of immunological tolerance and exocrine dysfunction in the salivary glands, providing a suitable platform to investigate the mechanisms regulating ELS formation and their role in the development of features typical of SS.

Supplementary Material

Refer to Web version on PubMed Central for supplementary material.

Acknowledgments

No conflict of interest pertinent to this article is declared. We thank Dr Luigi Gnudi, Professor of Diabetes and Metabolic Medicine, Unit for Metabolic Medicine, Cardiovascular Division, King's College London for proving us with the LacZ AdV.

REFERENCES

1. Drayton DL, Liao S, Mounzer RH, Ruddle NH. Lymphoid organ development: from ontogeny to neogenesis. Nat Immunol. 2006; 7:344–353. [PubMed: 16550197]
2. Aloisi F, Pujol-Borrell R. Lymphoid neogenesis in chronic inflammatory diseases. Nat Rev Immunol. 2006; 6:205–217. [PubMed: 16498451]
3. Manzo A, Bombardieri M, Humby F, Pitzalis C. Secondary and ectopic lymphoid tissue responses in rheumatoid arthritis: from inflammation to autoimmunity and tissue damage/remodeling. Immunol Rev. 2010; 233:267–285. [PubMed: 20193005]
4. Routsias JG, Tzioufas AG, Moutsopoulos HM. The clinical value of intracellular autoantigens B-cell epitopes in systemic rheumatic diseases. Clin Chim Acta. 2004; 340:1–25. [PubMed: 14734193]
5. Chisholm DM, Mason DK. Labial salivary gland biopsy in Sjogren's disease. J Clin Pathol. 1968; 21:656–660. [PubMed: 5697370]
6. Jonsson MV, Skarstein K, Jonsson R, Brun JG. Serological implications of germinal center-like structures in primary Sjogren's syndrome. J Rheumatol. 2007; 34:2044–2049. [PubMed: 17787040]
7. Barone F, Bombardieri M, Manzo A, Blades MC, Morgan PR, Challacombe SJ, Valesini G, Pitzalis C. Association of CXCL13 and CCL21 expression with the progressive organization of lymphoid-like structures in Sjogren's syndrome. Arthritis Rheum. 2005; 52:1773–1784. [PubMed: 15934082]
8. Xanthou G, Polihronis M, Tzioufas AG, Paikos S, Sideras P, Moutsopoulos HM. "Lymphoid" chemokine messenger RNA expression by epithelial cells in the chronic inflammatory lesion of the salivary glands of Sjogren's syndrome patients: possible participation in lymphoid structure formation. Arthritis Rheum. 2001; 44:408–418. [PubMed: 11229473]
9. Amft N, Curnow SJ, Scheel-Toellner D, Devadas A, Oates J, Crocker J, Hamburger J, Ainsworth J, Mathews J, Salmon M, Bowman SJ, Buckley CD. Ectopic expression of the B cell-attracting chemokine BCA-1 (CXCL13) on endothelial cells and within lymphoid follicles contributes to the establishment of germinal center-like structures in Sjogren's syndrome. Arthritis Rheum. 2001; 44:2633–2641. [PubMed: 11710719]
10. Bombardieri M, Barone F, Humby F, Kelly S, McGurk M, Morgan P, Challacombe S, De Vita S, Valesini G, Spencer J, Pitzalis C. Activation-induced cytidine deaminase expression in follicular dendritic cell networks and interfollicular large B cells supports functionality of ectopic lymphoid neogenesis in autoimmune sialoadenitis and MALT lymphoma in Sjogren's syndrome. J Immunol. 2007; 179:4929–4938. [PubMed: 17878393]

11. Salomonsson S, Jonsson MV, Skarstein K, Brokstad KA, Hjelmstrom P, Wahren-Herlenius M, Jonsson R. Cellular basis of ectopic germinal center formation and autoantibody production in the target organ of patients with Sjogren's syndrome. Arthritis Rheum. 2003; 48:3187–3201. [PubMed: 14613282]
12. Le Pottier L, Devauchelle V, Fautrel A, Daridon C, Saraux A, Youinou P, Pers JO. Ectopic germinal centers are rare in Sjogren's syndrome salivary glands and do not exclude autoreactive B cells. J Immunol. 2009; 182:3540–3547. [PubMed: 19265132]
13. Theander E, Vasaitis L, Baecklund E, Nordmark G, Warfvinge G, Liedholm R, Brokstad K, Jonsson R, Jonsson MV. Lymphoid organisation in labial salivary gland biopsies is a possible predictor for the development of malignant lymphoma in primary Sjogren's syndrome. Ann Rheum Dis. 2011; 70:1363–1368. [PubMed: 21715359]
14. Gatumu MK, Skarstein K, Papandile A, Browning JL, Fava RA, Bolstad AI. Blockade of lymphotoxin-beta receptor signaling reduces aspects of Sjogren's syndrome in salivary glands of non-obese diabetic mice. Arthritis Res Ther. 2009; 11:R24. [PubMed: 19222863]
15. Bombardieri M, Pitzalis C. Ectopic lymphoid neogenesis and lymphoid chemokines in Sjogren's syndrome: at the interplay between chronic inflammation, autoimmunity and lymphomagenesis. Curr Pharm Biotechnol. 2012
16. Smeets RL, van de Loo FA, Arntz OJ, Bennink MB, Joosten LA, van den Berg WB. Adenoviral delivery of IL-18 binding protein C ameliorates collagen-induced arthritis in mice. Gene Ther. 2003; 10:1004–1011. [PubMed: 12776157]
17. Reed LJ, Muench H. A simple method for estimating fifty percent endpoints. Am J Hyg. 1938; 27:493–497.
18. Correia PN, Carpenter GH, Paterson KL, Proctor GB. Inducible nitric oxide synthase increases secretion from inflamed salivary glands. Rheumatology (Oxford). 2010; 49:48–56. [PubMed: 19933597]
19. Astorri E, Bombardieri M, Gabba S, Peakman M, Pozzilli P, Pitzalis C. Evolution of ectopic lymphoid neogenesis and in situ autoantibody production in autoimmune nonobese diabetic mice: cellular and molecular characterization of tertiary lymphoid structures in pancreatic islets. J Immunol. 2010; 185:3359–3368. [PubMed: 20713891]
20. Samuni Y, Baum BJ. Gene delivery in salivary glands: from the bench to the clinic. Biochim Biophys Acta. 2011; 1812:1515–1521. [PubMed: 21763423]
21. Browning JL, Allaire N, Ngam-Ek A, Notidis E, Hunt J, Perrin S, Fava RA. Lymphotoxin-beta receptor signaling is required for the homeostatic control of HEV differentiation and function. Immunity. 2005; 23:539–550. [PubMed: 16286021]
22. Luther SA, Lopez T, Bai W, Hanahan D, Cyster JG. BLC expression in pancreatic islets causes B cell recruitment and lymphotoxin-dependent lymphoid neogenesis. Immunity. 2000; 12:471–481. [PubMed: 10843380]
23. Ngo VN, Korner H, Gunn MD, Schmidt KN, Riminton DS, Cooper MD, Browning JL, Sedgwick JD, Cyster JG. Lymphotoxin alpha/beta and tumor necrosis factor are required for stromal cell expression of homing chemokines in B and T cell areas of the spleen. J Exp Med. 1999; 189:403–412. [PubMed: 9892622]
24. Dawson LJ, Stanbury J, Venn N, Hasdimir B, Rogers SN, Smith PM. Antimuscarinic antibodies in primary Sjogren's syndrome reversibly inhibit the mechanism of fluid secretion by human submandibular salivary acinar cells. Arthritis Rheum. 2006; 54:1165–1173. [PubMed: 16572451]
25. Humphreys-Beher MG, Peck AB. New concepts for the development of autoimmune exocrinopathy derived from studies with the NOD mouse model. Arch Oral Biol. 1999; 44(Suppl 1):S21–25. [PubMed: 10414851]
26. Aziz KE, McCluskey PJ, Wakefield D. Characterisation of follicular dendritic cells in labial salivary glands of patients with primary Sjogren syndrome: comparison with tonsillar lymphoid follicles. Ann Rheum Dis. 1997; 56:140–143. [PubMed: 9068290]
27. Bombardieri M, Barone F, Pittoni V, Alessandri C, Conigliaro P, Blades MC, Priori R, McInnes IB, Valesini G, Pitzalis C. Increased circulating levels and salivary gland expression of interleukin-18 in patients with Sjogren's syndrome: relationship with autoantibody production and

lymphoid organization of the periductal inflammatory infiltrate. Arthritis Res Ther. 2004; 6:R447–456. [PubMed: 15380044]

28. Stott DI, Hiepe F, Hummel M, Steinhauser G, Berek C. Antigen-driven clonal proliferation of B cells within the target tissue of an autoimmune disease. The salivary glands of patients with Sjogren's syndrome. J Clin Invest. 1998; 102:938–946. [PubMed: 9727062]
29. Fleck M, Kern ER, Zhou T, Lang B, Mountz JD. Murine cytomegalovirus induces a Sjogren's syndrome-like disease in C57Bl/6-lpr/lpr mice. Arthritis Rheum. 1998; 41:2175–2184. [PubMed: 9870874]
30. Fleck M, Zhang HG, Kern ER, Hsu HC, Muller-Ladner U, Mountz JD. Treatment of chronic sialadenitis in a murine model of Sjogren's syndrome by local fasL gene transfer. Arthritis Rheum. 2001; 44:964–973. [PubMed: 11315936]
31. Nguyen CQ, Yin H, Lee BH, Carcamo WC, Chiorini JA, Peck AB. Pathogenic effect of interleukin-17A in induction of Sjogren's syndrome-like disease using adenovirus-mediated gene transfer. Arthritis Res Ther. 2010; 12:R220. [PubMed: 21182786]
32. van de Pavert SA, Mebius RE. New insights into the development of lymphoid tissues. Nat Rev Immunol. 2010; 10:664–674. [PubMed: 20706277]
33. Marinkovic T, Garin A, Yokota Y, Fu YX, Ruddle NH, Furtado GC, Lira SA. Interaction of mature CD3+CD4+ T cells with dendritic cells triggers the development of tertiary lymphoid structures in the thyroid. J Clin Invest. 2006; 116:2622–2632. [PubMed: 16998590]
34. Barone F, Bombardieri M, Rosado MM, Morgan PR, Challacombe SJ, De Vita S, Carsetti R, Spencer J, Valesini G, Pitzalis C. CXCL13, CCL21, and CXCL12 expression in salivary glands of patients with Sjogren's syndrome and MALT lymphoma: association with reactive and malignant areas of lymphoid organization. J Immunol. 2008; 180:5130–5140. [PubMed: 18354239]
35. Campbell AE, Cavanaugh VJ, Slater JS. The salivary glands as a privileged site of cytomegalovirus immune evasion and persistence. Med Microbiol Immunol. 2008; 197:205–213. [PubMed: 18259775]
36. Kloover JS, Hillebrands JL, de Wit G, Grauls G, Rozing J, Bruggeman CA, Nieuwenhuis P. Rat cytomegalovirus replication in the salivary glands is exclusively confined to striated duct cells. Virchows Arch. 2000; 437:413–421. [PubMed: 11097367]
37. Mariette X, Gottenberg JE. Pathogenesis of Sjogren's syndrome and therapeutic consequences. Curr Opin Rheumatol. 2010; 22:471–477. [PubMed: 20671520]
38. Tzioufas AG, Kapsogeorgou EK, Moutsopoulos HM. Pathogenesis of Sjogren's syndrome: What we know and what we should learn. J Autoimmun. 2012
39. Thaunat O, Patey N, Caligiuri G, Gautreau C, Mamani-Matsuda M, Mekki Y, Dieu-Nosjean MC, Eberl G, Ecochard R, Michel JB, Graff-Dubois S, Nicoletti A. Chronic rejection triggers the development of an aggressive intragraft immune response through recapitulation of lymphoid organogenesis. J Immunol. 2010; 185:717–728. [PubMed: 20525884]
40. Muramatsu M, Sankaranand VS, Anant S, Sugai M, Kinoshita K, Davidson NO, Honjo T. Specific expression of activation-induced cytidine deaminase (AID), a novel member of the RNA-editing deaminase family in germinal center B cells. J Biol Chem. 1999; 274:18470–18476. [PubMed: 10373455]
41. Dorner T, Radbruch A. Selecting B cells and plasma cells to memory. J Exp Med. 2005; 201:497–499. [PubMed: 15728231]
42. Manser T. Textbook germinal centers? J Immunol. 2004; 172:3369–3375. [PubMed: 15004133]
43. Recher M, Berglund LJ, Avery DT, Cowan MJ, Gennery AR, Smart J, Peake J, Wong M, Pai SY, Baxi S, Walter JE, Palendira U, Tangye GA, Rice M, Brothers S, Al-Herz W, Oettgen H, Eibel H, Puck JM, Cattaneo F, Ziegler JB, Giliani S, Tangye SG, Notarangelo LD. IL-21 is the primary common gamma chain-binding cytokine required for human B-cell differentiation in vivo. Blood. 2011; 118:6824–6835. [PubMed: 22039266]
44. Schneider P, MacKay F, Steiner V, Hofmann K, Bodmer JL, Holler N, Ambrose C, Lawton P, Bixler S, Acha-Orbea H, Valmori D, Romero P, Werner-Favre C, Zubler RH, Browning JL, Tschopp J. BAFF, a novel ligand of the tumor necrosis factor family, stimulates B cell growth. J Exp Med. 1999; 189:1747–1756. [PubMed: 10359578]

45. Castigli E, Wilson SA, Scott S, Dedeoglu F, Xu S, Lam KP, Bram RJ, Jabara H, Geha RS. TACI and BAFF-R mediate isotype switching in B cells. J Exp Med. 2005; 201:35–39. [PubMed: 15630136]

46. Xu W, He B, Chiu A, Chadburn A, Shan M, Buldys M, Ding A, Knowles DM, Santini PA, Cerutti A. Epithelial cells trigger frontline immunoglobulin class switching through a pathway regulated by the inhibitor SLPI. Nat Immunol. 2007; 8:294–303. [PubMed: 17259987]

47. Bombardieri M, Kam NW, Brentano F, Choi K, Filer A, Kyburz D, McInnes IB, Gay S, Buckley C, Pitzalis C. A BAFF/APRIL-dependent TLR3-stimulated pathway enhances the capacity of rheumatoid synovial fibroblasts to induce AID expression and Ig class-switching in B cells. Ann Rheum Dis. 2011; 70:1857–1865. [PubMed: 21798884]

48. Jonsson R, Vogelsang P, Volchenkov R, Espinosa A, Wahren-Herlenius M, Appel S. The complexity of Sjogren's syndrome: novel aspects on pathogenesis. Immunol Lett. 2011; 141:1–9. [PubMed: 21777618]

Europe PMC Funders Author Manuscripts

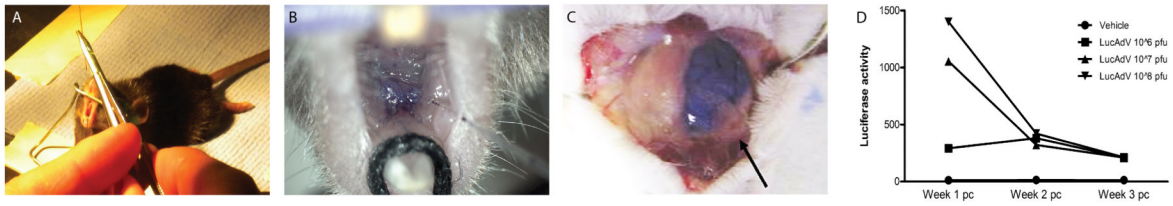

Figure 1. Efficiency of transfection following AdV delivery via retrograde mouse submandibular gland excretory duct cannulation

A-B) A glass cannula is inserted in the excretory orifice of the submandibular gland of a 12 weeks-old C57BL/6 mouse. **C)** Representative picture of a cannulated NOD mouse demonstrating that delivery of 50μl of bromophenol blue dye is sufficient to permeate the cannulated submandibular gland with no spillage to the contralateral gland or the adjacent sublingual gland (arrow). **D)** Representative dose-response time-course experiments of luciferase activity following delivery of LucAdV at 10^6, 10^7 and 10^8pfu/gland and vehicle control showing dose-dependent enzymatic activity within the first week. Dose dependency is lost at week 2 and 3 despite persistent transgene expression.

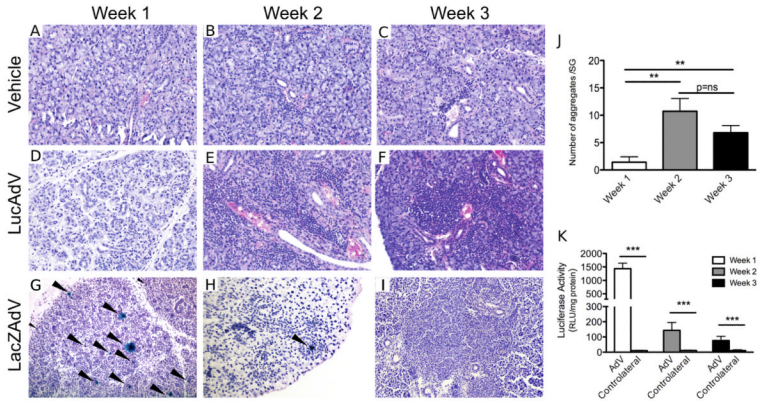

Figure 2. AdV delivery and its persistence in ductal epithelial cells progressively induce SS-like periductal inflammatory foci in wild-type C57BL/6 mice

A-F) Representative microphotographs showing inflammatory responses induced by local administration of either vehicle (***A-C***), LucAdV (***D-F***) or LacZAdV (***G-I***). After AdV delivery, diffuse lymphomonocytic infiltration in the first week (***D, G***) is followed by progressive organization of periductal inflammatory aggregates during week 2 (***E, H***) and week 3 pc (***F, I***). Vehicle delivery induces negligible inflammation (***A-C***). The mean ± SEM of the number of periductal foci/gland following either LucAdV or LacZAdV delivery at different time points is reported in J. (**p<0.01 between AdV and vehicle-treated mice at each time point, minimum of 10 mice per time point).

G-I) Representative microphotographs of submandibular glands infected with LacZAdV and stained for beta-galactosidase (XGal, with nuclear counterstaining with haematoxylin). Numerous beta-galactosidase-positive cells are present in the gland within the first week pc (***G,*** arrowheads). By week 2 pc only ductal epithelial cells, often surrounded by periductal inflammatory infiltrates, show enzymatic activity (***H***). By week 3 pc no residual XGal-positive cells are detectable (***I***) but high sensitivity luciferase activity assay in LucAdV-infected glands shows persistent signal well above background levels up to three weeks pc (***K,*** mean ± SEM of luciferase activity. Original magnification in A-I x100. (***p<0.001 between AdV-treated and vehicle-treated mice at each time point, minimum of 10 mice per time point).

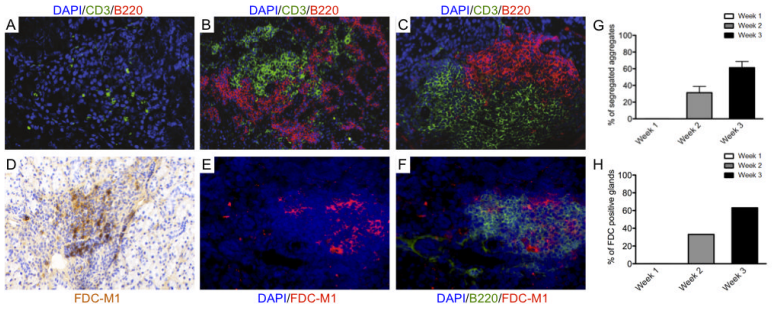

Figure 3. Progressive development of T/B cell segregation and FDC networks following AdV infection in the submandibular glands of C57BL/6 mice

A-C) Microphotographs showing double immunofluorescent staining for CD3 (T cells, in green) and B220 (B cells, in red) of frozen sections from AdV-treated C57BL/6 salivary glands. Nuclei are counterstained with DAPI (blue). Early diffuse infiltration is dominated by T cells (***A***) with subsequent recruitment of B cells showing initial T/B cell compartmentalization within the first 2 weeks pc (***B***). By week 3 pc over 60% of periductal foci display full segregation of T and B cells in separate areas (***C*** and ***G***).

D-F) Microphotographs of AdV-treated C57BL/6 submandibular glands at week 3 pc showing differentiation of FDC networks as demonstrated by staining for FDC-M1 (***D***, in brown and ***E*** in red). FDC networks invariably develop in the context of the B cell rich area of the aggregates (***F***) in over 60% of AdV-treated C57BL/6 mice (***H***). Original magnification x200.

Europe PMC Funders Author Manuscripts

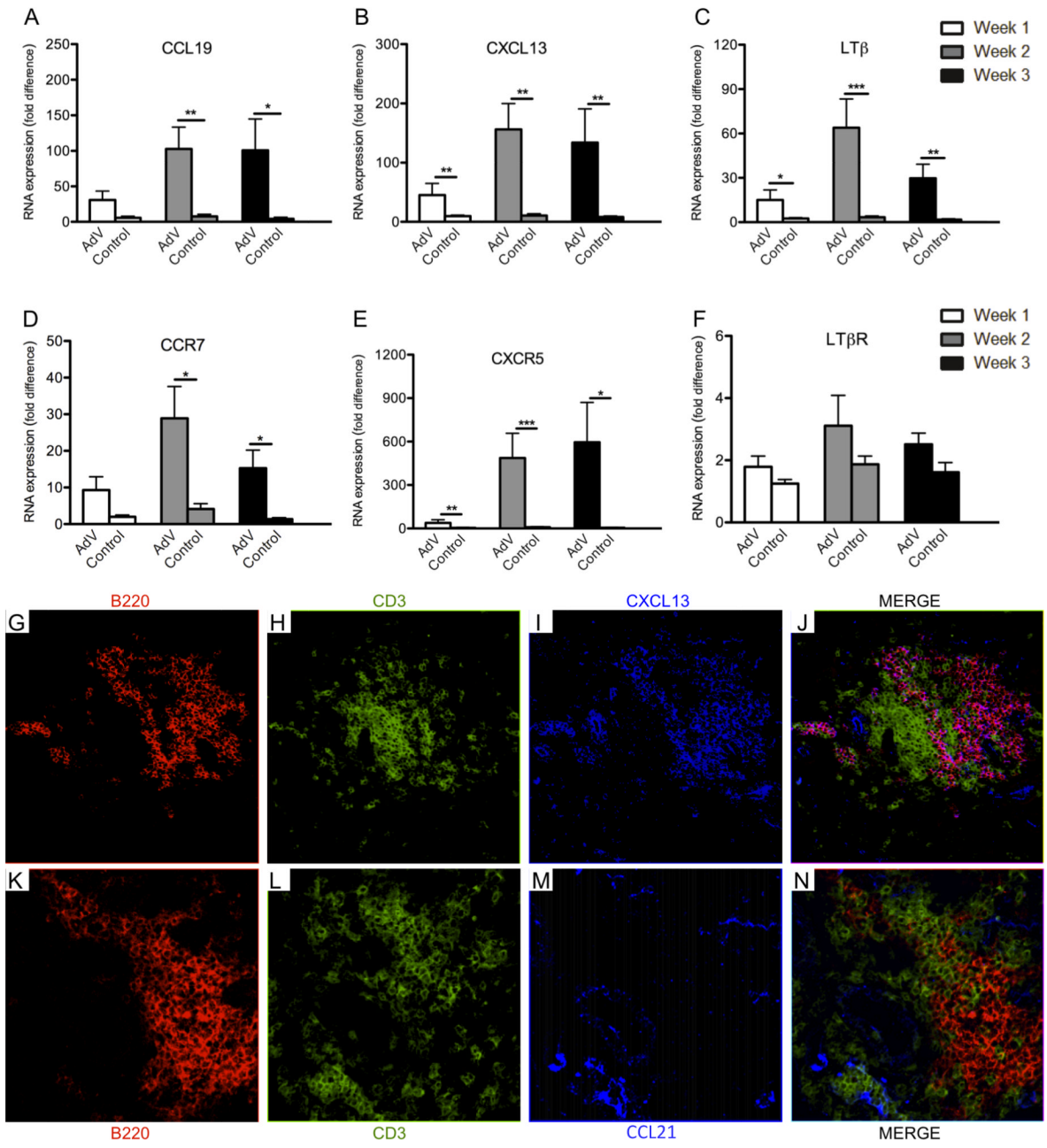

Figure 4. Development of ELS in C57BL/6 submandibular glands is preceded by ectopic expression of the lymphoid chemokines/Ltβ pathway

A-F) Quantitative TaqMan real-time PCR time-course analysis of CCL19 (and its receptor CCR7, ***A,D***) CXCL13 (and its receptor CXCR5, ***B,E***), and Ltβ(and its receptor, ***C,F***) mRNA transcripts showing abundant up-regulation following AdV-delivery in the submandibular glands. Earliest upregulation was observed for CXCL13 and Ltβ mRNA while peak of expression of these factors was detectable in parallel with full histological development of ELS (***A-E***). Conversely, LtβR expression appears unaffected by AdV treatment (***F***). Data are expressed as mean ± SEM of the fold-increase compared to an

internal calibrator. (*p<0.05, **p<0.01 and ***p<0.001 between AdV-treated and vehicle-treated mice at each time point, minimum of 10 mice per time point).
G-N) Microphotographs of multi-color confocal microscopy analysis confirming protein expression of lymphoid chemokines CXCL13 (***I,*** in blue) and CCL21 (***M***) and showing co-localization of CXCL13 within the B cell-rich area (***G-J***) and of CCL21 within the T cell rich area of the aggregate (***K-N)*** B cells are shown in red (CD19) and T cells in green (CD3), respectively. Original magnification x200.

Europe PMC Funders Author Manuscripts

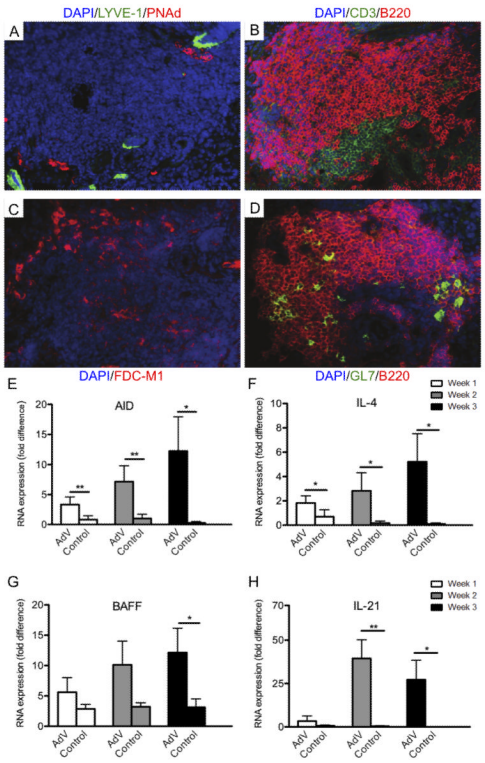

Figure 5. AdV-induced ELS in C57BL/6 submandibular glands acquire characteristics of functional ectopic germinal centers

A-D) Sequential immunofluorescence staining of AdV-treated submandibular gland sections of C57BL/6 mice at 3 weeks pc showing that highly organized ELS characterized by high-endothelial venules (HEV, ***A*** in red), T/B cell segregation (***B***, B220 in red and CD3 in green) and FDC networks (***C***) support the differentiation of GL7+ germinal center B cells (***D***, B220 in red and GL7 in green).

E-H) Quantitative TaqMan real-time PCR time-course analysis of salivary gland expression of AID mRNA (***E***) and transcripts for cytokines downstream AID activation, such as IL-4, BAFF and IL-21 (***F-H***). AID expression peaks in parallel with the development of fully formed ELS and is associated with significant upregulation of IL-4, BAFF and IL-21. Data are expressed as mean ± SEM of the fold-increase compared to an internal calibrator. (*p<0.05 and **p<0.01 between AdV-treated and vehicle-treated mice at each time point, minimum of 10 mice per time point). Original magnification X200 (A-D).

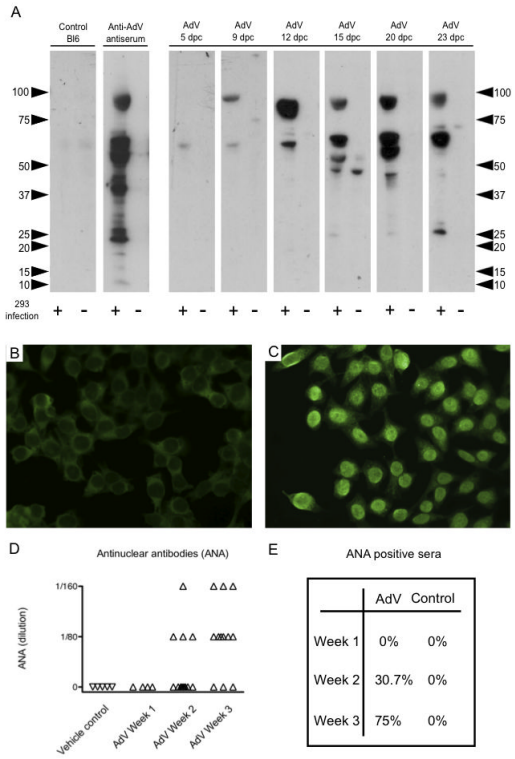

Figure 6. Development of anti-viral and anti-nuclear antibodies following AdV delivery in the submandibular glands of C57BL/6 mice

A) Western blot showing progressive development of anti-AdV IgG in the serum of AdV-treated but not vehicle-cannulated mice. Protein extracts from AdV-infected (+) and uninfected (−) 293 cells were run in parallel. From left to right: vehicle-treated C57BL/6 mouse serum at 20 days pc, commercial anti-AdV antiserum, sera from AdV-cannulated mice at different time-points (5, 9, 12, 15, 20, 23 days pc). Anti-AdV responses are observed as early as day 5 pc and are mainly directed against proteins of the viral core and capside. **B-E)** Representative microphotographs of immunofluorescent detection of anti-nuclear antibodies (ANA) using Hep2 cells as substrate (***B,C***) demonstrating strong nuclear reactivity in sera of AdV-treated (***C***) but not in vehicle-cannulated (***B***) C57BL/6 mice 3 weeks pc (dilution 1:80). ANA reactivity was progressively evident over time in AdV-cannulatedC57BL/6 mice (***D***) with 75% of mice displaying ANA positivity by week 3 pc (***E***). Original magnification X400 (B-C).

Europe PMC Funders Author Manuscripts

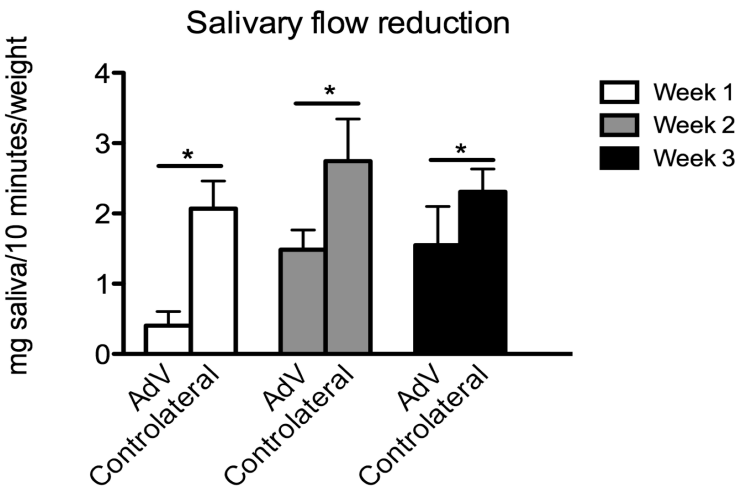

Figure 7. Sustained reduction in salivary flow following AdV infection of C57BL/6 mice submandibular glands

Column graphs comparing salivary flow in the AdV-treated submandibular and the contralateral gland at week 1, 2 and 3 pc. Salivary flow is measured as mg of saliva produced in 10 minutes/body weight following pilocarpine stimulation (see methods). Exocrine dysfunction in the AdV-cannulated glands can be observed up to three weeks pc. Data are expressed as mean ± SEM. (*$p<0.05$ between AdV-treated and vehicle-treated mice at each time point, minimum of 5 mice per time point).

Europe PMC Funders Author Manuscripts

Table I

List of primary and secondary antibodies used for immunofluorescence

Clone/Catalog N.	Specificity	Host	Source
500A2	Biotin anti-mouse CD3ε	Hamster	BD Pharmingen
RA3-6B2	PE anti-mouse B220	Rat	BD Pharmingen
MECA-79	Biotin anti-mouse PNAd	Rat	Biolegend
AF2125	Anti-mouse Lyve-1	Goat	R&D Systems
FDC-M1	Anti-mouse FDC	Rat	BD Pharmingen
AF470	Anti-mouse CXCL13	Goat	R&D Systems
AF457	Anti-mouse CCL21	Goat	R&D Systems
S-32354	Streptavidin Alexa 488		Invitrogen
S-32355	Streptavidin Alexa 555		Invitrogen
A-11078	Anti-goat Alexa 488	Rabbit	Invitrogen
A-21434	Anti-rat Alexa 555	Goat	Invitrogen
A-11034	Anti-rabbit 488	Goat	Invitrogen
A-11090	Anti-FITC	Rabbit	Invitrogen
A-11055	Anti-goat Alexa 488	Donkey	Invitrogen

Europe PMC Funders Author Manuscripts

Table II

List of primers and probes for Taqman real-time PCR

Gene product	mRNA Acc. number	Assay Id	Source
Mouse AID	NM_009645	Mm00507774_m1	Applied Biosystems
Mouse CXCL13	NM_018866	Mm00444533_m1	Applied Biosystems
Mouse CXCR5	NM_007551	Mm00432086_m1	Applied Biosystems
Mouse CCL19	NM_011888	Mm00839967_g1	Applied Biosystems
Mouse CCR7	NM_007719	Mm00432608_m1	Applied Biosystems
Mouse BAFF	NM_033622	Mm00446347_m1	Applied Biosystems
Mouse IL-4	NM_021283	Mm00445259_m1	Applied Biosystems
Mouse IL-21	NM_021782	Mm00517640_m1	Applied Biosystems
Mouse LTβ	NM_008518	Mm00434774_g1	Applied Biosystems
Mouse LTβR	NM_010736	Mm00440235_m1	Applied Biosystems
Eukaryotic 18S		Cat N 4319413E	Applied Biosystems